

DNA Conformational Switches as Sensitive Electronic Sensors of Analytes

Richard P. Fahlman and Dipankar Sen*

Contribution from the Department of Molecular Biology and Biochemistry,
Simon Fraser University, Burnaby, British Columbia V5A 1S6, Canada

Received November 29, 2001

Abstract: The electrical conductivity of DNA is dependent on its conformational state. We demonstrate here that such a dependence may be harnessed for the electronic sensing of external analytes, for instance, adenosine. Such a DNA sensor incorporates an analyte “receptor”, whose altered conformation in the presence of bound analyte switches the conformation, and hence, the conductive path between two DNA double-helical stems. Two distinct designs for such sensors are described here, that permit significant electrical conduction through a “detector” double-helical stem only in the presence of the bound analyte. In the first design, current flows through the analyte receptor itself, whereas in the second, current flows in a path adjacent to the receptor. The former design may be especially suitable for certain categories of analytes, including heterocycle-containing compounds such as adenosine, whereas the latter design should be generally applicable to the detection of any molecular analyte, large or small. Since analyte detection in these DNA sensors is electronic, the potential exists for their application in rapid and automated chip-based detection of small molecules as well as of proteins and other macromolecules.

Introduction

Despite a lack of complete understanding of the mechanistic details of electron transfer through DNA, long-range electron transfer in double-stranded DNA is generally believed to be the result of a multistep hopping reaction.^{1–2} Studies on long-range electron transfer through DNA, however, have generated a consensus that a continuous base-stacking throughout a DNA duplex is essential. Efficiency of charge transfer is reduced in duplexes containing mismatches^{3–5} and bulges.⁶ Proteins that bind and disrupt continuous base-stacking in duplex DNA also reduce the efficiency of electron transfer past the site of helix disruption.^{7–8} Despite the importance of a continuous base stack, not all perturbations to the helix prevent charge transfer, as it has been observed in helices containing abasic sites⁹ and through short, single-stranded overhangs.¹⁰ However, even these latter structures are believed to base-stack, which permits charge transfer through them.

In nature, DNA is known to bind a variety of small molecule as well as macromolecular ligands. However, recent innovations

in vitro selection (SELEX) methods have resulted in DNA (as well as RNA) “aptamer” sequences, which are capable of specifically binding a variety of molecular species, including many that normally do not interact with DNA or RNA.¹¹ Such aptamer oligonucleotides frequently exhibit induced-fit folding behavior (reviewed by Hermann and Patel¹²), whereby the aptamer itself, largely unstructured in solution, undergoes significant compaction and structural stabilization upon binding its cognate ligand.

Our strategy for sensor design utilized a trial analyte, adenosine, which binds poorly, if at all, to double-stranded DNA but for which a high-affinity ($K_d \approx \mu\text{M}$) DNA aptamer sequence has been derived.¹³ NMR studies have confirmed that this aptamer, upon binding two molecules of adenosine, shows a typical adaptive folding, forming a tightly hydrogen-bonded and stacked helical structure.¹⁴ Figure 1 illustrates two distinct, albeit related, conceptions of DNA sensors for the analyte adenosine: in the first (*upper*), analyte binding directly closes an impaired double-helical path and facilitates electron transfer through this path. Such a device might be termed an “integrated-ligand” sensor. A more versatile conception (Figure 1, *lower*) is that of a “coupled-ligand sensor”, in which analyte binding to a receptor (aptamer) site adjacent to a distorted double-helical path leads to a lessening of the distortion and an enhanced electron flow through the path. In the “integrated” sensor, the adenosine/ATP aptamer loop separates the Watson–Crick base paired “AQ” and “Detector” double-helical stems, interrupting the continuous

* To whom correspondence should be addressed. Telephone: 604-291-4386. Fax: 604-291-5583. E-mail: sen@sfu.ca.

- (1) Giese, B. *Acc. Chem. Res.* **2000**, *33*, 631–636.
- (2) Schuster, G. B. *Acc. Chem. Res.* **2000**, *33*, 253–260.
- (3) Kelly, S. O.; Holmlin, R. E.; Stemp, E. D. A.; Barton, J. K. *J. Am. Chem. Soc.* **1997**, *119*, 9861–9870.
- (4) Giese, B.; Wessely, S. *Angew. Chem., Int. Ed.* **2000**, *39*, 3490–3491.
- (5) Boon, E. M.; Ceres, D. M.; Drummond, T. G.; Hill, M. G.; Barton, J. K. *Nature Biotechnol.* **2000**, *18*, 1096–1100.
- (6) Hall, D. B.; Barton, J. K. *J. Am. Chem. Soc.* **1997**, *119*, 5045–5046.
- (7) Rajski, S. R.; Kumar, S.; Roberts, R. J.; Barton, J. K. *J. Am. Chem. Soc.* **1999**, *121*, 5615–5616.
- (8) Rajski, S. R.; Barton, J. K. *Biochemistry* **2001**, *40*, 5556–5564.
- (9) Gasper, S. M.; Schuster, G. B. *J. Am. Chem. Soc.* **1997**, *119*, 12762–12771.
- (10) Kan, Y.; Schuster, G. B. *J. Am. Chem. Soc.* **1999**, *121*, 10857–10864.

- (11) Gold, L.; Polisky, B.; Uhlenbeck, O.; Yarus, M. *Annu. Rev. Biochem.* **1995**, *64*, 763–797.
- (12) Herman, T.; Patel, D. J. *Science* **2000**, *287*, 820–825.
- (13) Huizenga, D. E.; Szostak, J. W. *Biochemistry* **1995**, *34*, 656–665.
- (14) Lin, C. H.; Patel, D. J. *Chem. Biol.* **1997**, *4*, 817–832.

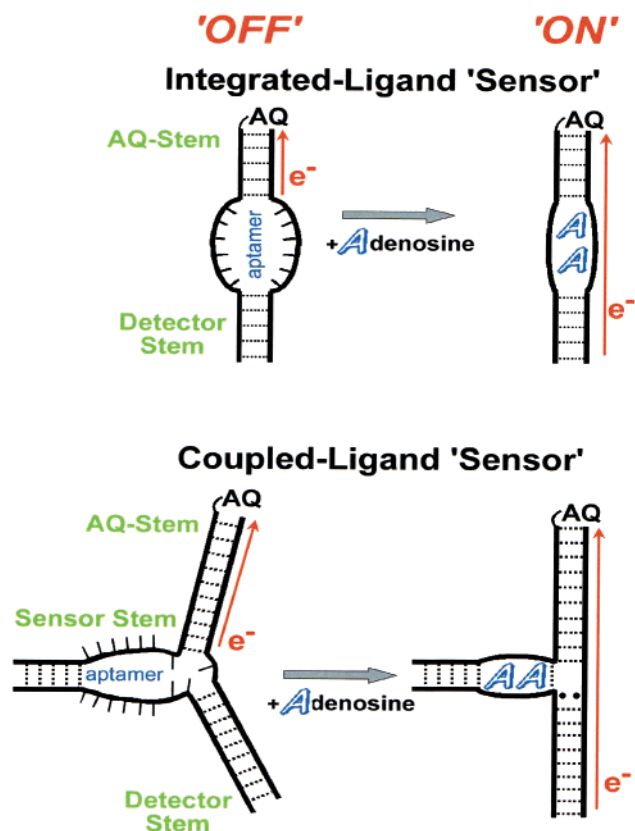


Figure 1. Design of the “integrated-ligand” and “coupled-ligand” sensors. In the absence of ligand/analyte (adenosine) both sensors adopt open, unstructured conformations, which only allow charge transfer (indicated by arrows) from the AQ stems. Adenosine binding induces the folding and compaction of the adenosine aptamer, facilitating charge transfer from the Detector stems.

helical path between them and, specifically, between individual bases in the Detector stem and the oxidant anthraquinone (AQ), tethered covalently to the end of the AQ stem. Here, the expectation was that the folding and internal stacking of the aptamer loop upon adenosine binding would facilitate electron flow between the AQ and the Detector stems. In the “coupled-ligand” sensor, however, the aptamer domain, adjacent to but separate from the electronic path, would act as a switch. Its ordered state, in the presence of adenosine, would change the stacking of the AQ and the Detector stems, thereby changing in the current flow through the Detector stem.

Materials and Methods

DNA Preparation. Unmodified DNA sequences were purchased from Sigma-Genosys and purified by PAGE before use. Sequences to be ^{32}P -end-labeled were pretreated with 10% piperidine (90 °C for 30 min followed by lyophilization) prior to 5'- ^{32}P -kinasing and PAGE purification. Such a pretreatment cleaved DNA molecules damaged during synthesis, leading in turn to lower background cleavages from photoirradiation experiments, as previously described.¹⁵

DNA sequences to be derivatized with anthraquinone were synthesized with a commercially available 5'-C6-amino functionality, and were purchased from the University of Calgary Core DNA Services. Generation of anthraquinone-modified DNA sequences was accomplished by reacting the *N*-hydroxysuccinimide ester of anthraquinone-2-carboxylic acid¹⁶ with the 5'-C6-amino functionality on the DNA.

Coupling and purification protocols were as described for amine reactive dyes by Molecular Probes¹⁷ with some modifications.

Prior to coupling, the DNA was treated to remove nitrogenous contaminants from the DNA synthesis procedures. The dried DNA samples were first suspended in 100 μL of ddH₂O, and were extracted three times with 100 μL of chloroform. The DNA remaining in the aqueous phase was then precipitated by the addition of 30 μL of 1 M NaCl and 340 μL of 100% EtOH. Following mixing, the sample was chilled on dry ice for ~ 10 min, and then centrifuged in a microfuge for 20 min to pellet the DNA. The pellet was washed once with 150 μL of 70% aqueous ethanol (v/v). Following air-drying the pellet was dissolved in 100 μL of ddH₂O, the DNA concentration of the solution was determined in a standard fashion using UV absorbance measurements.

The AQ-NHS ester (4.8 mg) was dissolved in 238 μL of dimethylformamide. For each coupling reaction, 7 μL of this stock suspension was added to 75 μL of a 100 mM sodium borate solution (pH 8.5). To the resulting mixture was added 8–15 μL (5–10 nmol) of the purified amino-labeled DNA. The tubes containing the coupling mixtures were covered in aluminum foil and shaken overnight at room temperature. The DNA was then ethanol-precipitated by addition of 27 μL of 1 M NaCl and 280 μL of 100% ethanol (the solution was chilled in dry ice and the precipitated DNA collected and washed as described above). The large pellet obtained (containing a significant amount of the uncoupled anthraquinone) was now suspended in 50 μL of 100 mM aqueous triethylamine acetate (pH 6.9) to which was added 100 μL of chloroform. The uncoupled anthraquinone partitioned into the chloroform phase, and the aqueous phase was now extracted two more times with 100 μL of chloroform, prior to partial drying under vacuum to remove any residual chloroform. The DNA obtained was then purified by reverse phase chromatography on an HPLC using a C18 Bondapak column (Waters).

The HPLC protocol was as follows: the solvent flow was continuous at 1 mL/minute, and the column was heated to 65 °C. The initial conditions were: 100% Solvent A (20:1 of 100 mM triethylamine acetate, pH 6.9:acetonitrile) changing to 30% Solvent B (100% acetonitrile), over 30 min and with a linear gradient. After this period, the solvent was rapidly changed to 100% Solvent B, for 15 min, before reconditioning the column to the starting conditions.

The concentrations of the various products of the coupling reactions could be determined spectroscopically. Absorbance values for the conjugate were made at 260 nm, using extinction coefficients for the individual bases obtained for single stranded DNA: ϵ (260 nm, $\text{M}^{-1}\text{cm}^{-1}$) adenine (A) = 15 000, guanine (G) = 12 300, cytosine (C) = 7400, thymine (T) = 6700, and anthraquinone (AQ) = 29 000. Typical yields of AQ–DNA conjugates ranged from 50 to 85%, depending on the sequence of the DNA oligonucleotide being coupled, and the synthetic batch.

Preparation of DNA Assemblies. DNA assemblies were formed by annealing mixtures of constituent DNA oligonucleotides (1 μM each) in 100 mM Tris-Cl, pH 7.9, and 0.2 mM EDTA. DNA solutions were heated to 90 °C for 2 min, and then cooled at a rate of 2 °C/minute to a final temperature of 20 °C. The solutions were then diluted 2-fold with either 5 mM MgCl₂ or 5 mM MgCl₂ and 200 mM NaCl (the final solutions being defined as the “Mg” and “Mg–Na” buffers, respectively). These solutions also contained 2 \times concentrations of adenosine or uridine in some samples. After mixing, the samples were incubated for approximately 30 min at room temperature before photo-irradiation.

Photoirradiation. Preincubated samples were placed under a UVP Black-Ray UVL-56 lamp (366 nm peak intensity, at 18 W) for 90 min at a distance of 4 cm from the bulb. Temperature was maintained by having the samples tubes placed in a water bath set to the desired temperature. Following photoirradiation, the samples were lyophilized and then treated with hot piperidine as described above. The treated

(15) Odom, D. T.; Dill, E. A.; Barton, J. K. *Chem. Biol.* **2000**, *7*, 475–481.

(16) Telsler, J.; Cruickshank, K. A.; Morrison, L. E.; Netzel, T. L.; Chan, K. J. *Am. Chem. Soc.* **1989**, *111*, 7226–7232.

(17) URL: <http://www.probes.com/media/pis/mp00143.pdf>.

between the constructs, however, were observed in cleavage at the distal (“D”) guanine doublet. In both the presence and absence of added nucleosides the control duplex exhibited identical levels of cleavage at the “D” guanines (lanes 4–6). However, the “integrated-ligand” sensor only exhibited significant cleavage at the “D” guanines in the presence of adenosine (lane 12), but not in the presence of uridine (lane 13), no added nucleoside (lane 11), or in a “dark” (i.e., unirradiated—lane 10) control. To test whether the cleavages observed arose uniquely from oxidation by the attached anthraquinone functionality, and also to test whether such putatively AQ-dependent cleavages occurred strictly in *intra*-molecular fashion, photoirradiation was carried out on samples containing mixtures of ^{32}P -end-labeled constructs lacking anthraquinone and unlabeled constructs conjugated to anthraquinone. Lanes 7 and 14 show that no significant cleavage in the labeled strands was observed, either for the double-stranded control or the integrated sensor construct.

The fact that in the integrated-ligand sensor high levels of strand cleavage were observed only at the proximal (“P”) guanine doublet in the presence of uridine (lane 13), as well as in the absence of added nucleosides (lane 11, Figure 3A), indicated that charge transport in these cases was localized almost exclusively within the AQ stem (as depicted in the model for this sensor in Figure 1). By contrast, when 2.5 mM adenosine was present (lane 12) the same experimental procedure resulted in 5.0% cleavage at the distal (“D”) guanine doublet (up from 0.26% shown in lanes 11 and 13) when photoirradiated for 90 min. This reflects a ~ 20 -fold enhancement in strand-cleavage in the presence of the adenosine ligand. This observation indicates that the adenosine-induced folded structure of the aptamer was indeed capable of facilitating charge transfer between the Detector and AQ stems. Interestingly, in the presence of adenosine, even the “P” doublet showed a small enhancement in cleavage (< 2 -fold), consistent with an overall tightening and stabilization of the sensor construct.

When experiments similar to the above were carried out in the absence of NaCl (i.e., in the “Mg” buffer: 50 mM Tris-Cl, pH 7.9, 2.5 mM MgCl_2 , and 0.1 mM EDTA), somewhat different results were observed (Figure 3B). The double-stranded control showed comparable cleavage patterns as seen in the “Mg–Na” buffer, that is, strand cleavage was observed at the proximal (P) and distal (D) guanine doublets both in the absence (lane 4) or presence (data not shown) of 2 mM adenosine (relative to the “dark” control—lane 3). By contrast, the integrated sensor construct exhibited significant strand cleavage at the distal (D) guanine doublet in the presence of 2 mM added adenosine (lane 12)—as also seen in the “Mg–Na” buffer (Figure 3A). This increase in strand cleavage, from 0.98 to 7.3%, describes a ~ 7 -fold enhancement in the presence of adenosine.

The major difference observed for the sensor construct in the “Mg” buffer (Figure 3B), relative to the “Mg–Na” buffer (Figure 3A), was that in the “Mg” buffer enhanced cleavage occurred at the proximal (P) guanine doublet in the presence of adenosine (lane 12 versus lanes 11 and 13, Figure 3B). This enhanced cleavage may reflect a proportionately greater stabilization of the duplex elements flanking the aptamer by the aptamer-bound adenosines in this relatively low-salt buffer. We believe that this enhanced proximal G cleavage was *not* a consequence of the reassociation of the strands of the sensor construct dissociated in the “Mg” buffer (nondenaturing gel

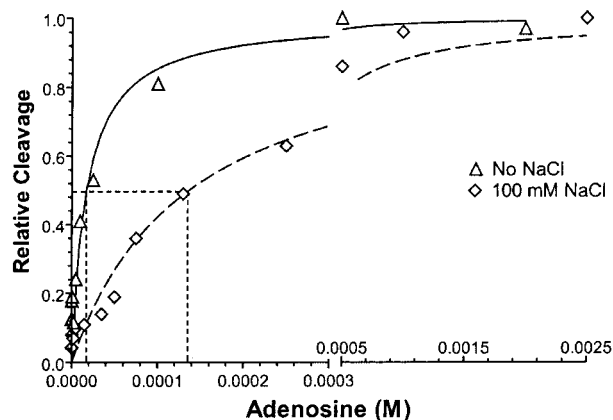


Figure 4. Adenosine-dependence of cleavage at the distal guanines of the “integrated-ligand” sensor construct. Samples of the sensor construct (0.5 μM) were photoirradiated for 90 min at 18 $^{\circ}\text{C}$ in either the “Mg” or “Mg–Na” buffer, in the presence of various adenosine concentrations. Following irradiation, samples were piperidine-treated and loaded on sequencing gels. Strand cleavage, quantitated in a phosphorimager, were corrected against “dark,” nonirradiated, controls and normalized for the maximal observed cleavage.

electrophoresis experiments showed that the constructs remained intact in all buffers and experimental conditions used in this study—data not shown).

Variations in solution conditions also affected the efficiency of strand cleavage at the distal (D) guanine doublet as a function of adenosine concentration. Figure 4 shows how in different solutions different binding affinities were observed for the adenosine ligand. In the “Mg” buffer, half-maximal strand cleavage was observed at 18 μM adenosine, while in the “Mg–Na” buffer, it was observed at 135 μM adenosine.

The Coupled-Ligand Sensor. We also examined the properties of a different sensor design, the “coupled-ligand” sensor (which also utilized the ATP aptamer, and is shown schematically in Figure 1, lower). This second design does not depend on the conductive property of the folded aptamer domain. The predicted lack of base stacking between the Sensor stem and either the AQ or the Detector stem in the folded state is expected to prevent electron transfer between these regions. A “coupled-ligand” sensor of this design, for detecting adenosine, was assembled from the DNA oligomers shown in Figure 5A. In this construct, the aptamer bulge was separated from the three-way junction by a single A–T base pair. To detect charge transfer in the various arms, the DNA strand shared by both the Sensor and Detector stems was 5′- ^{32}P -labeled. Figure 5B shows the results obtained when samples were irradiated in the “Mg–Na” buffer for 180 min. In the absence of added adenosine (lane 5), or in the presence of 2.5 mM uridine, no detectable cleavage above the background level (lane 6) was observed at all positions. In the presence of 2.5 mM adenosine (lane 4), however, significantly enhanced strand cleavage (> 15 -fold enhancement in replicate experiments) was seen at the 5′-guanine of each of the two-guanine doublets present in the Detector stem (indicated as *x* and *y*). Lack of detectable cleavage at these guanines in the absence of adenosine prevented the determination of an absolute ratio for cleavage enhancement; however, the lower limit indicated above (> 15 -fold) could be calculated. A comparable enhancement, however, was not observed for the doublet (*z*) located in the Sensor stem (2–4-fold increase) as predicted by our structural model of this DNA

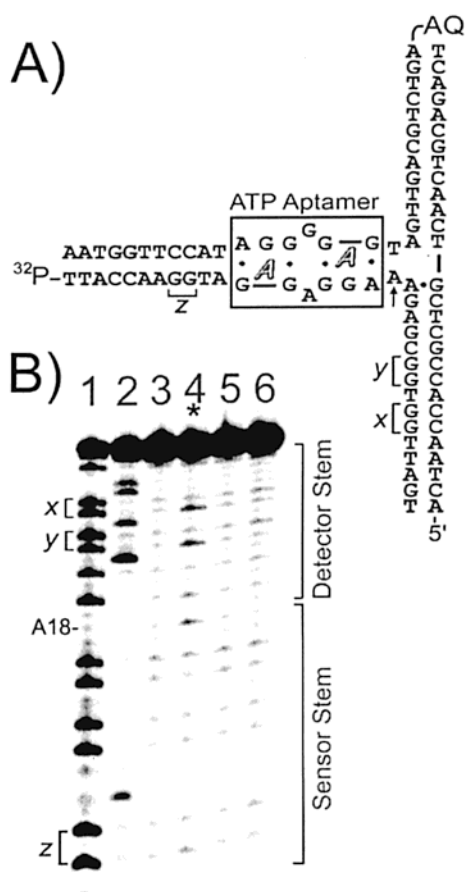


Figure 5. Charge transfer in the “coupled-ligand” sensor. (A) The structure and sequence of the “coupled-ligand” sensor. The ATP aptamer domain is indicated as boxed, while the two bound adenosines are indicated by outlined “A”s. Guanine doublets in the 5′-³²P-end labeled strand used to monitor charge transfer to the Sensor and Detector stems are indicated as “x”, “y”, and “z”. The A•G mismatch at the junction was used since it gave superior results relative to Watson–Crick base pairs at that position. The arrow, on an adenine at the junction, indicates an adenine that showed an unusually high cleavage (see lane 4, below). (B) Phosphorimager traces of strand-cleavage data from the “coupled-ligand” sensor construct, irradiated at 18 °C for 180 min in the “Mg–Na” buffer. Lanes 3–5 show cleavage results in the presence of 2.5 mM uridine (lane 3); 2.5 mM adenosine (lane 4); and, buffer alone (lane 5). Lanes 1 and 2 show the Maxam–Gilbert “G” and “C+T” ladders, respectively. Lane 6 shows the background piperidine cleavage of the nonirradiated construct.

construct. Irradiation experiments on a control construct for the above three-way junction that lacked the aptamer bulge but incorporated a Watson–Crick duplex (as with the “integrated sensor”—see above) in place of the aptamer “arm” yielded no modulation of strand cleavage in the presence of added adenosine (data not shown).

The effect of different buffer conditions on strand cleavage in this construct was not examined, as nondenaturing electrophoresis experiments indicated that this sensor construct was not sufficiently stable structurally in the low-salt “Mg” buffer (data not shown).

Discussion

Experiments with the above two sensor designs, utilizing the ATP aptamer as a “sensing” receptor, clearly demonstrate the utility of DNA conformational changes (resulting from the adaptive binding of ligand to the DNA aptamer) in modulating charge transfer through DNA.

Investigations with the integrated-ligand sensor, above, have demonstrated that both the sensitivity of and signal enhancement from analyte-sensing depend significantly on solution conditions. It is still unclear whether such differences reflect purely structural transformations of the aptamer in the different ionic-strength solutions or whether they also reflect changes in the process of charge transfer through DNA.

Comparison of the behavior of the integrated sensor in the two ionic-strength conditions tested indicates a tradeoff between signal enhancement and sensitivity. In the relatively low-salt “Mg” buffer a half-maximal enhancement of ~ 3.5 -fold enhanced cleavage at the distal (“D”) guanine doublet was observed with 18 μM adenosine, whereas in the higher salt Mg–Na buffer a half-maximal enhancement of ~ 10 -fold was observed with 130 μM adenosine. In other words, the addition of 100 mM NaCl generated a highly amplified signal, but at the cost of a lower sensitivity of adenosine detection. Such an unusual trend may result from the aptamer forming a subtly altered structure under higher ionic-strength conditions, one that requires higher adenosine concentrations to drive the equilibrium to the adenosine-bound form. The guanine-rich aptamer domain could potentially form foldback G–G base pairs or guanine quartets in the presence of NaCl.^{24–25} In fact, guanine quartets were originally postulated to be a part of the folded aptamer structure when the aptamer was originally identified.¹³

In addition, care must be taken in interpreting the results of the adenosine-dependence data from Figure 4, since the curves may not directly reflect the binding affinities of the aptamer for its ligand. As described above, each molecule of this particular aptamer binds two molecules of the adenosine ligand, and it is unclear whether the binding of only one molecule of ligand allows charge transfer to occur to some extent.

Comparing the efficiencies of conduction through particular DNA sequences has often been accomplished by comparing the ratios of cleavage at “proximal” and “distal” guanines (D/P or P/D ratios).^{7,8,19,26,27} This comparison is an indicator of the efficiency with which charge transfer proceeds through a specified sequence of interest that is flanked by isolated guanines, doublets, triplets, or reactive bases such as 8-oxoguanine⁹ or 7-deazaguanine.²⁷ A comparison of conduction through the integrated sensor and through its double-stranded control gave D/P ratios, respectively, of 0.48 ± 0.07 versus 0.23 ± 0.04 in the “Mg–Na” buffer and 0.4 ± 0.08 versus 0.24 ± 0.05 in the “Mg” buffer. Comparing these ratios at face value suggests that the aptamer domain is a somewhat superior conductor compared to the double-stranded DNA control. However, direct comparisons of the sensor and the duplex control may not be entirely appropriate. When irradiation experiments were carried out such that comparable levels of strand cleavage were achieved at the distal (“D”) guanine doublets in both the control and sensor constructs, a 2-fold higher cleavage was observed at the proximal (“P”) guanine doublet of the double stranded control. The reduced efficiency of cleavage at the proximal guanines in the sensor construct must reflect a hindrance to charge migration into sequences

(24) Wellinger, R.; Sen, D. *Eur. J. Cancer* **1997**, *33*, 735–749.

(25) Simonsson, T. *Biol. Chem.* **2001**, *382*, 621–628.

(26) Giese, B.; Amaudrut, J.; Kohler, A. K.; Spormann, M.; Wessely, S. *Nature* **2001**, *412*, 318–320.

(27) Nakatani, K.; Dohno, C.; Saito, I. *J. Am. Chem. Soc.* **2000**, *122*, 5893–5894.

influenced by the presence of the aptamer, given that the double-stranded proximal stems are identical in both the sensor and double-stranded constructs. Once a mobile charge reaches the proximal (“P”) guanine doublet, it then appears that the “integrated-ligand” sensor better facilitates the transfer of that charge to the distal (“D”) guanine doublet in comparison to the double-stranded control. A possible reason for the lower D/P ratios seen in the duplex control may result from the GG doublets situated between the “P” and “D” doublets on the AQ-modified strand (Figure 2). These intervening doublets may be acting as “traps”, thus reducing the efficiency of charge transfer to the distal (“D”) guanine doublet of the duplex control. Overall, it is still remarkable that the folded, *non*-B-DNA aptamer possesses a comparable if not more favorable conductive property than the B-DNA duplex control.

In addition to the capacity of the ATP aptamer to modulate charge transfer between the acceptor and detector stems, interesting observations were made regarding the aptamer domain, specifically. Cleavage at the guanines located *within* the aptamer domain was observed to be low in both of the buffers used (Figure 3, A and B, lanes 11–13). Low cleavage in the absence of bound adenosine was reduced further upon the binding of adenosine. This observation may reflect the non-B helical structure of the folded aptamer domain. The high level of oxidation of the 5'-most guanine in guanine doublets is strictly true only for double-stranded B-DNA.²⁸ Single-stranded sequences,¹⁰ and guanine quadruplexes,²⁹ for instance, do not show this pattern. This property of the aptamer guanines may explain the lower D/P ratio of the sensor, relative to that of the duplex control.

The demonstrated capacity of the DNA aptamer for adenosine/ATP to act as a conduit for charge transfer in the folded state is a property not likely shared by all aptamer motifs. In addition to inherent conductivity differences between different aptamers, some aptamers, which are not formed from internal (bulge) loops, may not easily be incorporated into duplex DNA. To design a more general sensor, capable of utilizing diverse receptors and aptamers and responding to a variety of ligands/analytes, an immobile three-way helical junction was used as a starting point for a second design. This “coupled-ligand” sensor (Figure 5A) also exhibited modulation of charge transfer from the Acceptor to Detector stems in response to adenosine binding to the aptamer element. This construct, however, required longer irradiation times (relative to that required for the integrated sensor) to obtain significant levels of cleavage at the guanine doublets (*x* and *y* in Figure 5A) in the Detector stem. It remains to be investigated whether the lower charge-transfer efficiency in the “coupled-ligand” construct arose from the particular sequences chosen for the stems or from the presence of the three-way junction. Future work will also focus on determining the three-dimensional structure of this three-way junction to understand why significantly more strand cleavage was observed in the Detector stem compared to that in the Sensor stem.

A deeper characterization of the “coupled-ligand” sensor design, and of related architectures, is desirable given their broad potential for development as modular sensors. In the “coupled-ligand” sensor there is only a requirement for a conformational

change in the analyte-binding (aptamer or receptor) domain upon the binding of the analyte, and *not* for an inherent ability of the binding domain to permit charge transfer through its own structure. The side-on placement of the analyte receptor should also be applicable in the design of hybrid sensors that are not composed entirely of DNA. Such hybrid systems may possess binding domains consisting of RNA, proteins or other organic “host” entities (such as crown ethers, cryptands, and others) that undergo a conformational change upon binding the appropriate “guest” molecule or ion.

The guanine damage- and electrophoresis-based detection methodology used in this contribution were necessary for single-nucleotide resolution investigations of the charge-conduction pathways in the sensors. Here, we have used them to demonstrate that ligand-induced conformational changes can indeed be used to modulate charge transfer through DNA. However, to develop this technology for the rapid detection of ligand molecules other detection methodologies will need to be employed. The most likely scenario would have the DNA sensor constructs functionalized onto metal or other surfaces such that direct measurements of current flow can be made. Reports of successful coupling of modified DNA to electrodes and the direct monitoring (by chemical reaction in solution or photo-excitation) of hybridization via charge transfer through the resulting duplex,^{5,30–31} suggests that aptamers can also be used in this way toward the development of novel DNA-based sensors.

For the applicability of this technology as a practical detection method, the sensitivity of detection must be sufficient. As described, the sensitivity of this system is limited by the affinity of the incorporated aptamer sequence for its target ligand (given that the magnitude of the signal is proportional to the fraction of sensor constructs bound with ligand). The ATP aptamer described in this report possesses a dissociation constant in the μM range for the adenosine ligand. Such a binding affinity would be insufficient for a practical sensor intended to monitor, for instance, hormone levels in blood (for which sensor–analyte affinities in the low-nM-to-high-pM range would be required). Binding affinities of the nM–pM range, however, are possible and have been obtained with nucleic acid aptamers; for example, an RNA aptamer selected for binding to the aminoglycoside antibiotic tobramycin, possessed a binding constant of 770 pM.³²

More broadly, the receptor component of such DNA sensors need not in itself be composed of DNA or RNA. Organic or inorganic hosts, which undergo significant conformational change upon binding their cognate guest could, in principle, be incorporated in place of DNA or RNA aptamers into the design of such sensors.

Conclusions

Here we have demonstrated that charge transfer can be modulated by conformational changes resulting from the adaptive binding of a DNA aptamer to its ligand. Our demonstration of two DNA architectures that successfully modulated charge transfer as the consequence of the binding of an analyte suggests

(28) Saito, I.; Takayama, M.; Sugiyama, H.; Nakatani, K.; Tsuchida, A.; Yamamoto, M. *J. Am. Chem. Soc.* **1995**, *117*, 6406–6407.

(29) Szalai, V.; Thorp, H. H. *J. Am. Chem. Soc.* **2000**, *122*, 4524–4525.

(30) Kelly, S. O.; Jackson, N. M.; Hill, M. G.; Barton, J. K. *Angew. Chem., Int. Ed.* **1999**, *38*, 941–945.

(31) Boon, E. M.; Ceres, D. M.; Drummond, T. G.; Hill, M. G.; Barton, J. K. *Nature Biotechnol.* **2000**, *18*, 1096–1100.

(32) Wang, Y.; Killian, J.; Hamasaki, K.; Rando, R. R. *Biochemistry* **1996**, *35*, 12338–12346.

that this methodology may be used in the development of a variety of electrically coupled analyte sensors.

Harnessing the potential of conformational switches in nucleic acids is a relatively new endeavor. It has been used, to date, in the development of a mechanical switch,³³ allosteric enzymes³⁴ and, now, electronic devices. The ability to monitor the presence

and concentration of analytes electrically promises the development of rapid, DNA-based, “solid-state” detection devices for virtually any compound.

Acknowledgment. We thank Ross Hill and Peter Unrau for helpful discussions. This work was funded by grants from NSERC Canada and CIHR Canada to D.S.; R.P.F. is an NSERC Postgraduate Scholar.

- (33) Mao, C.; Sun, W.; Shen, Z.; Seeman, N. C. *Nature* **1999**, *397*, 144–146.
(34) Soukup, G. A.; Breaker, R. R. *Curr. Opin. Struct. Biol.* **2000**, *10*, 318–325.

JA012618U